Proceedings of the XI Bulgarian-Serbian Astronomical Conference (XI BSAC) Belogradchik, Bulgaria, May 14-18, 2018
Editors: Milcho K. Tsvetkov, Milan S. Dimitrijević and Momchil Dechev,
Publ. Astron. Soc. "Rudjer Bošković" No 18, 2018, 117-125

HARD X-RAY DIAGNOSTIC OF PROTON PRODUCING SOLAR FLARES COMPARED TO OTHER EMISSION SIGNATURES

ROSITSA MITEVA[1], KOSTADINKA KOLEVA[2], MOMCHIL DECHEV[2], ASTRID VERONIG[3], KAMEN KOZAREV[2], MANUELA TEMMER[3], KARIN DISSAUER[3] and PETER DUCHLEV[2]

[1]*Space Research and Technology Institute, Bulgarian Academy of Sciences Acad. Georgi Bonchev Str., Block 1, 1113 Sofia, Bulgaria*
[2]*Institute of Astronomy with National Astronomical Observatory, 72 Tsarigradsko Chaussee Blvd., 1784 Sofia, Bulgaria*
[3]*Institute of Physics/IGAM, University of Graz, Universitätsplatz 5, A-8010 Graz, Austria*
E-mail: rmiteva@space.bas.bg, koleva@astro.bas.bg, mdechev@astro.bas.bg, astrid.veronig@uni-graz.at, kkozarev@astro.bas.bg, manuela.temmer@uni-graz.at, karin.dissauer@uni-graz.at, pduchlev@astro.bas.bg

Abstract. We present results on the correlation analysis between the peak intensity of the in situ proton events from SOHO/ERNE instrument and the properties of their solar origin, solar flares and coronal mass ejections (CMEs). Starting at the RHESSI mission launch after 2002, 70 flares well-observed in hard X-rays (HXRs) that are also accompanied with in situ proton events are selected. In addition to HXRs, flare emission at several other wavelengths, namely in the soft X-ray (SXR), ultraviolet (UV) and microwave (MW), is used. We calculated Pearson correlation coefficients between the proton peak intensities from one side, and, from another, the peak flare flux at various wavelengths or the speed of the accompanied CME. We obtain the highest correlations with the CME speed, with the SXR flare class and with MWs, lower ones with the SXR derivative, UV and 12–50 keV HXRs and the lowest correlation coefficients are obtained with the 50–300 keV HXRs. Possible interpretations are discussed.

1. INTRODUCTION

The quest towards the solar origin of in situ observed solar energetic particles (SEPs: electrons, protons and heavy ions at energies above keV, Desai and Giacalone, 2016) is still ongoing after multiple decades of research (Basilevskaya, 2017). From one side, the main mechanisms for particle acceleration out of

thermal populations in the solar corona are well known: magnetic reconnection and shock waves (Klein and Dalla, 2017). The eruptive processes on the Sun where both of these acceleration processes take place are solar flares (SFs) and coronal mass ejections (CMEs). However, the individual contribution of SFs and CMEs to the in situ detected particle flux is unknown. The initial general consensus of predominant acceleration by flares later shifted to the expectation that CMEs cause most, if not all, of the particle acceleration (when CMEs were discovered). Further work led to the impulsive vs. gradual SEP classification doctrine (Reames 1999), but after several proposed modifications (e.g., Cliver 2009), consensus finally settled on the mixed-origin contribution standpoint (e.g., Cane et al. 2010 and references therein). Although, both, SFs and CMEs are nowadays accepted to accelerate SEPs, their individual contributions to the observed particle flux event are hard to separate. The standard procedure when dealing with a large sample of events is to calculate Pearson correlation coefficients between the peak proton flux (or an integrated value, fluence) and some characteristic value for the SF (i.e., flare class, fluence and rise time) and CME (i.e., linear speed and angular width), usually adopted from catalogs (see discussion in Dierckxsens et al. 2015). Several guiding principles must be considered in the SEP research, e.g., the big flare syndrome (Kahler 1982) and the longitudinal effect on the particle profiles and intensities (e.g., Lario et al. (2013) for multi-spacecraft observations).

Solar flare intensity is defined as the peak value (measured in W/m^2) in the 1–8 Å channel (i.e., soft X-rays, SXRs) observed by GOES satellites (https://satdat.ngdc.noaa.gov/sem/goes/data/). The wavelength is representative of thermal emission. SXR data is freely provided by the GOES team since the 1970s, and this energy channel is nowadays used for the definition of SF class (from so-called A (being a multiplication factor of 10^{-8}) to X (10^{-4}) flare class). The electromagnetic (EM) emission during (especially large) SFs could span from the gamma to radio range (Benz 2002, 2017, Fletcher 2011). The light-curve, depending on the wavelength, has specific time profile, duration, acceleration mechanism, emission site in the solar atmosphere, etc. In this study we use SXR, hard X-ray (HXR), ultraviolet (UV) and radio data.

With the launch of the RHESSI satellite in 2002 (until its decommissioning in 2018), HXRs and gamma-rays from solar flares have routinely been measured according to the observing mode of the spacecraft (Lin et al. 2002). The HXR instrument observes flare emission from 3 keV up to 20 MeV as counts per seconds. Different models can be subsequently applied to reconstruct the HXR photon flux from the measured count rates.

Previous studies relating HXRs and proton events are reported by Kiplinger (1995), with a focus on the spectral properties of the flares using Solar Maximum mission (SMM) data. The study started with selection of 152 HXR flares, well-observed with SMM, and explored their link to interplanetary proton events. The study concluded that absence of flare spectral hardening is associated (to over 95%) to the absence of proton events and vice versa (82%). In a second analysis,

193 less intense flares, compared to the first sample, were used to successfully predict occurrence of large proton events.

The recent state of the art instrument in the extreme- and ultraviolet (EUV and UV, respectively) range is the Atmospheric Imaging Assembly (AIA) aboard the Solar Dynamics Observatory (SDO; Lemen et al. 2012). AIA observes the Sun in 10 wavelengths with a cadence as high as 12 seconds.

In the radio domain we use data from the Radio Station Telescope Network (RSTN, Guidice et al. 1981) which is a set of four nearly identical stations (located in Learmonth – Western Australia, San Vito – Southern Italy, Sagamore Hill – Massachusetts, USA and Palehua – Hawaii, USA). The temporal coverage is nearly complete. Observations at eight discrete frequencies from 245 MHz to 15.4 GHz are routinely done with 1-second time resolution. Radio flux density is observed in solar flux units (sfu). For the purpose of this analysis (favoring signatures of non-thermal emission) we use the highest available frequency, 15.4 GHz, falling in the microwave (MW) range.

The aim of the present study is to statistically investigate new EM wavelengths as alternatives of the well-known SXR flux using Pearson correlation analysis widely used to quantify the solar origin of SEP events. Adopting HXRs as a reference emission, all other wavelengths are the EM signatures of the proton-producing HXR flares.

2. DATA AND ANALYSIS

For the current study we used in situ protons in the 17–22 (~20) MeV energy channel of SOHO/ERNE instrument (Torsti et al. 1995). The proton events are identified in the period 1996–2017 (Miteva and Danov 2018) and constitute the reference channel of an on-line catalog under development (Miteva 2017, Miteva and Danov 2017): **http://newserver.stil.bas.bg/SEPcatalog/**. About 660 proton events are identified at present. An example of the proton time profile is presented in Miteva (2017).

In addition, temporal and longitudinal association between the proton events and the solar eruptive phenomena, occurring prior the SEP increase at 1 AU, is performed. Namely a pair (where possible) of flare and CME are assigned as the most probable origin to each proton event (see Miteva 2017 for the details of the adopted procedure). The number of solar associations is always reduced with respect to the total number of identified proton enhancements.

The so-identified list of solar flares (close to 400 flares) is subsequently used to firstly check if the flare is observed by the RHESSI satellite using the RHESSI browser 2.0 tool (**http://sprg.ssl.berkeley.edu/~tohban/browser/**) – see examples in Fig. 1. Due to the rotation and orbit characteristics of the satellite, periods of observations are interrupted by night time and passage through the South Atlantic Anomaly. This fact reduced drastically the number of detected flare events. As additional condition, HXR data should be available during the observations at least from the onset to the peak of the emission at several HXR channels. Thus, a

list of 70 events with protons and flare HXR emission is finally compiled in the present analysis.

Complementary to the RHESSI HXRs, we use the standard wavelength used in the definition for the flare class and provided by the GOES 1–8 Å SXR channel. In addition we use SDO/AIA 1600 Å channel (sensitive to upper photosphere and transition region) and RSTN 15.4 GHz microwaves (radio emission from the lower layers of the solar atmosphere). As an example, we show the light curves for the 15-Feb-2011 flare: X2.2 in SXR GOES class (provided by the quick-look RHESSI browser, Fig. 1 left), RHESSI HXRs (3–300 keV, Fig. 1 right), SDO/AIA UV (Fig. 2 left) and RSTN MWs (Fig. 2 right). SXR and UV are smooth peaks, whereas HXR and MW emission show more bursts.

Each proton event in our list is also linked to a CME (unless there is a data gap or the association is uncertain). For comparative purposes, we perform correlations between the proton peak intensity and the linear speed of the CMEs adopted here from the SOHO LASCO CME catalog (https://cdaw.gsfc.nasa.gov/CME_list/).

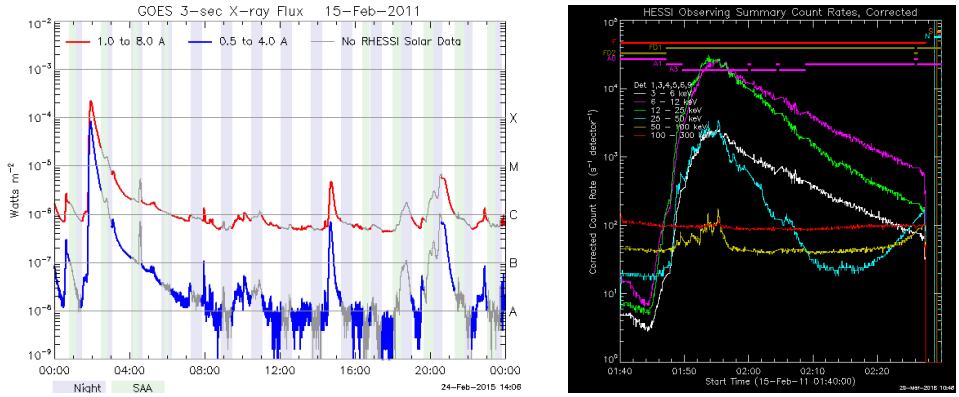

Figure 1: Example for 15-Feb-2011 solar flare observations in GOES SXRs (left) and RHESSI corrected count rates at several energy channels (right).

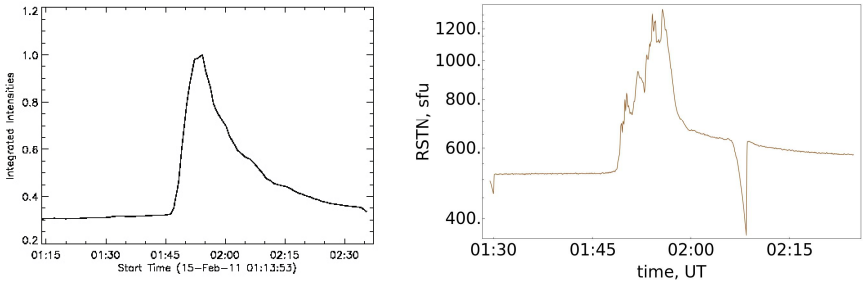

Figure 2: Examples for the 15-Feb-2011 flare light curves in 1600 Å UV (left) and 15.4 GHz MW (right) wavelengths. The abrupt drop in the declining MW phase is a data artifact.

3. RESULTS

The following procedure for the analysis of all EM curves (HXR, SXR, UV and MW) is performed. We first calculate background subtracted amplitudes. The analysis starts with a manual selection of the start and end times of the quiet-time intensity. The intensity over this period is averaged to give the (pre-event) background level for each flare. The latter value is subsequently subtracted from the identified peak value (i.e., from the highest intensity level of the light-curve). A similar procedure is applied also to the proton data to calculate the SEP proton peak fluxes.

The number of events used further are as follows: 70 events for 12–25 keV HXRs and SXR flare class; the SXR derivative could be calculated for all but one case; with the increase of the energy, the event sample is reduced to 64 events with HXR signal in 25–50 keV, 55 – in 50–100 keV to only 34 events with 100–300 keV HXRs. Similarly, radio data at 15.4 GHz is found for 50 events and UV data is available only for 22 events (mostly due to the SDO/AIA coverage).

Since the time derivative of SXR is commonly used as an approximation for the HXRs, so-called Neupert effect (Dennis and Zarro, 1993, Veronig et al. 2005), we performed a cross-correlation between the values for the GOES derivative and the RHESSI count rates in 4 different energy channels (Fig. 3). Pearson correlation coefficient is calculated, as well as an uncertainty using the bootstrapping method (Wall and Jenkins, 2003). The largest values for the correlations are obtained for the 'softest|' HXR 12–25 MeV (0.93±0.02) and 25–50 MeV (0.82±0.06) channels, being reduced greatly at the harder HXRs, 50–100 keV (0.57±0.12) and 100–300 keV (0.45±0.18). The event number for each calculation is limited to the sample size of the higher HXR energy in each pair.

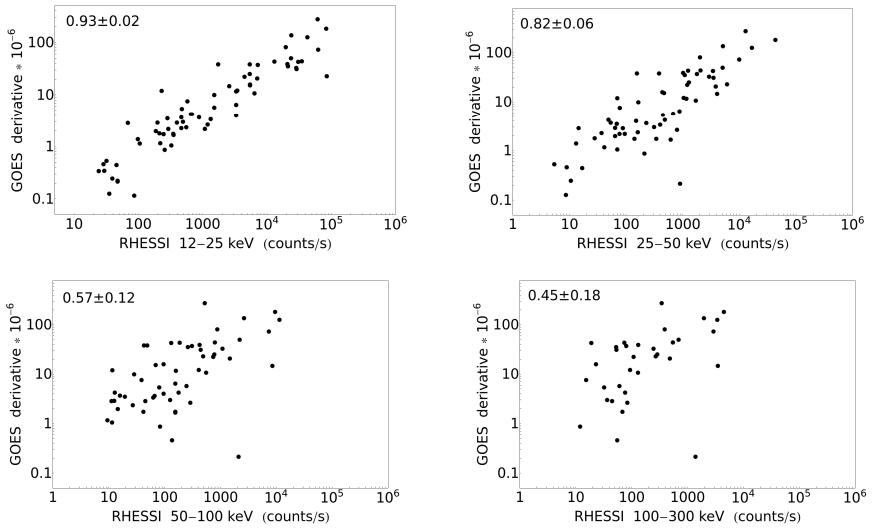

Figure 3: Scatter plots of GOES SXR derivative and RHESSI count rates in different energy channels.

Table 1: Correlation coefficients between the ~20 MeV SOHO/ERNE peak proton intensity and the properties of flare EM emission and CME speed. The number of events used in each calculation is given in brackets. See text for abbreviations used.

	Correlation coefficients	
Solar origin properties	***All events***	***Well-connected events***
Flare EM emission		
SXR 1–8 Å, W/m^2	0.56±0.09 (70)	0.61±0.09 (52)
SXR derivative, W/(m^2 s)	0.48±0.09 (69)	0.50±0.10 (52)
HXR 12–25 keV, counts/s	0.48±0.08 (70)	0.50±0.10 (51)
HXR 25–50 keV, counts/s	0.50±0.09 (64)	0.50±0.11 (47)
HXR 50–100 keV, counts/s	0.44±0.11 (55)	0.38±0.13 (41)
HXR 100–300 keV, counts/s	0.41±0.12 (34)	0.42±0.13 (28)
MW 15.4 GHz, sfu	0.55±0.10 (50)	0.62±0.11 (35)
UV 1600 Å, relative units	0.50±0.15 (22)	0.43±0.20 (15)
CME speed, km/s	**0.64±0.08 (65)**	**0.72±0.07 (50)**

The main objective of the analysis is the calculation of the Pearson correlation coefficients between the peak proton intensity at ~20 MeV and the EM emission amplitudes at each wavelength under consideration. For the purpose of comparison, we also used the speed of the CME. All results are summarized in Table. 1 and several of the examples are explicitly shown as scatter plots in Fig. 4.

We performed the log10–log10 correlations for the entire sample ('All events') and for a subset of events that fulfill the condition to originate from western helio-longitudes (or so-called here 'Well-connected events'). The sample is dominated by well-connected events (i.e., originating from western helio-longitudes, denoted with filled circles in Fig. 4, whereas the remaining cases are eastern events – plotted in open circles, respectively) which is a well-known property of SEP events. With the exception of two wavelengths (HXR 50–100 keV and UV 1600 Å) the correlation coefficients are higher (or the same, as for HXR 25–50 keV) for the well-connected events compared to the entire sample. Since the uncertainty ranges are fairly large, the improvement is, however, not statistically significant.

The standard correlation used to quantify the solar origin contribution to the proton flux is between the proton peak intensity with the SF class and/or with the CME linear speed. The correlations with the CMEs is slightly better (0.64±0.08) compared to the SXR flare class (0.56±0.09) considering the (nearly) entire event list. The same trend is kept also for the well-connected sample. Again, the differences are within the error bars.

The correlation coefficients obtained between the proton peak flux and SXR derivative, as well as between the proton flux and HXR peak value at 12–25 keV are very similar. When using the higher energy channel 25–50 keV the values are still very close to those with the SXR derivative. This is due to the highest cross-

correlation between the two types of data (Fig. 3). Considering the highest energy channels used here (>50 keV) for the HXRs, we obtained smaller values for the correlation coefficients (the lowest for the 100–300 keV HXRs, 0.41±0.12), compared to the SXRs and statistically lower (especially for the western events) than those with the CME speed. The number of events at 100–300 keV is also reduced compared to the initial sample size, which also increases the uncertainty. The respective values for the MWs are very similar to the SXRs, (0.55±0.10), or slightly lower when using UV data (0.50±0.12).

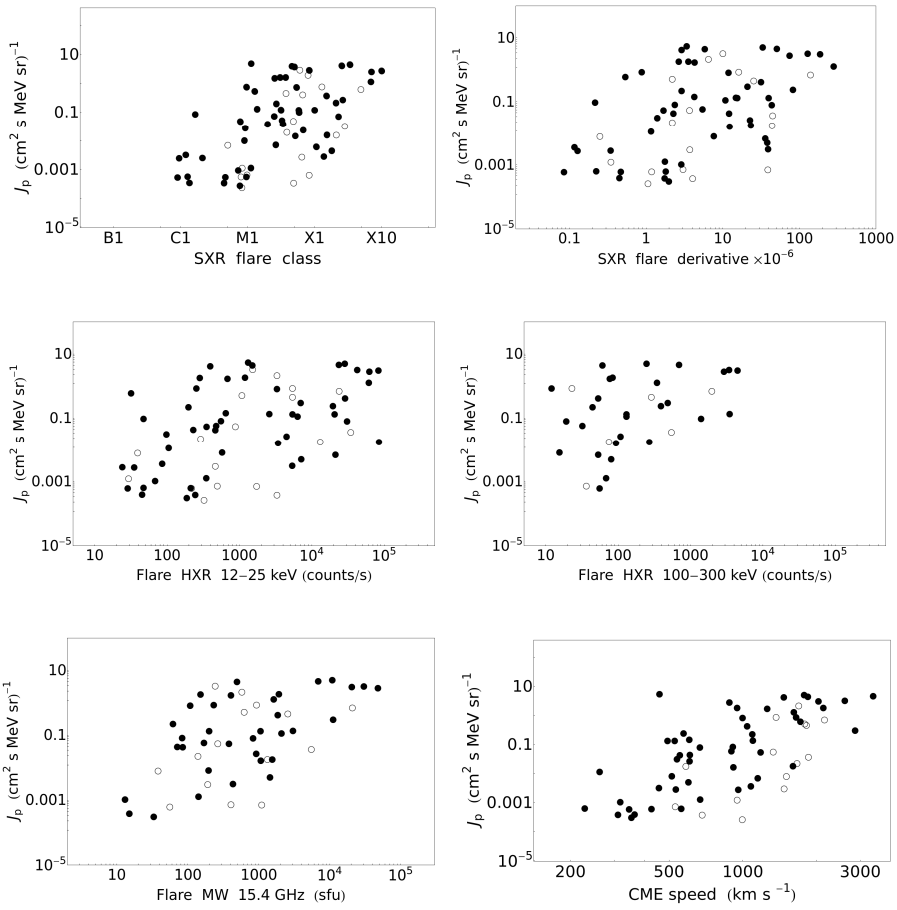

Figure 4: Selected scatter plots of the ~20 MeV peak proton intensity (J_p) and the properties of flare EM emission and/or CME speed. Open circles denote events originating from eastern helio-longitudes, filled circles – western origin events.

4. DISCUSSION

The use of non-thermal flare signatures compared to SXRs when performing correlations with in situ SEP flux is the main objective in this study. Moreover, here we applied different selection criteria compared to Kiplinger (1995), namely we started with a list of in situ proton events identified from ~20 MeV SOHO/ERNE data, performed association with SXR flares and then searched for the HXR signatures. The final number of SFs (reduced to only 70) is primarily due to the observing mode of the HXR instrument used.

HXR emission signatures are a more adequate choice to explore non-thermal particle acceleration processes taking place in SFs compared to thermal SXRs. We used the simplest way (corrected count rates) to quantify the light curves in different energy bands provided by the RHESSI satellite. Lower correlations between the >50 keV HXR count rates and the proton peak intensity as compared to the SXR flare class and CME speed are found. In contrast, when using MW (known to temporarily correlate better with HXRs) and UV emission we obtain results closer to those of SXRs.

A possible reason for the obtained correlation trends could be either a reduced contribution or efficiency drop of the SF acceleration process (in terms of HXR emission) to the in situ proton flux. Alternatively, the sample of 70 events could be biased due to the observational selectivity of the HXR instrument. Both possibilities should be further explored. Moreover, using the peak value of the SXR emission (so-called flare class) could lead to an overestimation of the SF influence to SEP events. In addition to the SF acceleration and emission, the energized particles need to escape the Sun and reach the detector, which could be suppressed, to a degree, in these events due to a specific magnetic field configuration.

An important forthcoming study to be performed is using HXR fluence instead of the peak value in the statistical analysis, as shown by Trottet et al. (2015) that SXR fluence should be used instead of the SXR class. Moreover, HXR flux, contrary to count rates, deduced in terms of model fitting is another step of a future analysis.

Acknowledgements

We acknowledge SOHO/ERNE, RHESSI, GOES, SDO/AIA and RSTN data in our study. SOHO is a project of international collaboration between ESA and NASA. This research is funded by a bilateral collaborative project under agreement between Bulgaria's National Science Fund NTS/AUSTRIA 01/23, 28.02.17 and Austria OeAD Project No. BG 11/2017.

References

Bazilevskaya, G. A.: 2017, *Journal of Physics: Conference Series*, **798 (1)**, 012034.

Benz, A.: 2002, *Plasma Astrophysics. Kinetic Processes in Solar and Stellar Coronae*, second edition. By A. Benz, Institute of Astronomy, ETH Zürich, Switzerland. *Astrophysics and Space Science Library*, **279**, Kluwer Academic Publishers, Dordrecht.

Benz, A. O.: 2017, *Living Reviews in Solar Physics*, **14 (1)**, 2.

Cane, H. V., Richardson, I. G., von Rosenvinge, T. T.: 2010, *Journal of Geophysical Research*, **115 (A8)**, A08101.

Cliver, E. W.: *Central European Astrophysical Bulletin*, **33**, 253–270.

Desai, M., Giacalone, J.: 2016, *Living Reviews in Solar Physics*, **13 (1)**, 3.

Dennis, B. R.; Zarro, D. M.: 1993, *Solar Physics*, **146 (1)**, 177–190

Dierckxsens, M., Tziotziou, K., Dalla, S., Patsou, I., Marsh, M. S., Crosby, N. B., Malandraki, O., Tsiropoula, G.: 2015, *Solar Physics*, **290 (3)**, 841–874.

Fletcher, L.; Dennis, B. R.; Hudson, H. S.; Krucker, S.; Phillips, K.; Veronig, A. et al.: 2011, *Space Science Reviews*, **159 (1/4)**, 19–106.

Guidice, D. A.; Cliver, E. W.; Barron, W. R.; Kahler, S.: 1981, *Bulletin of the American Astronomical Society*, **13**, 553.

Kahler, S. W.: 1982, *Journal of Geophysical Research*, **87**, 3439–3448.

Kiplinger, A. L.: 1995, *The Astrophysical Journal*, **453**, 973–986.

Klein, K.-L., Dalla, S.: 2017, *Space Science Reviews*, **212 (3/4)**, 1107–1136.

Lario, D., Aran, A., Gómez-Herrero, R., Dresing, N., Heber, B., Ho, G. C., Decker, R. B., Roelof, E. C.: 2013, *The Astrophysical Journal*, **767 (1)**, 41.

Lemen, J. R., Title, A. M., Akin, D. J., Boerner, P. F., Chou, C.; Drake, J. F. et al.: 2012, *Solar Physics*, **275 (1-2)**, 17–40.

Lin, R. P., Dennis, B. R., Hurford, G. J., Smith, D. M., Zehnder, A., Harvey, P. R. et al.: 2002, *Solar Physics*, **210 (1)**, 3–32.

Miteva, R.: 2017, Thirteenth International Scientific conference "Space, Ecology, Safety - SES", held 2-4 November 2017 in Sofia, Bulgaria, edited by G. Mardirossian, Ts. Srebrova and G. Jelev, ISSN: 1313-3888, 52–56.

Miteva, R.; Danov, D.: 2017, Ninth Workshop 'Solar Influences on the Magnetosphere, Ionosphere and Atmosphere', proceedings of the conference held 30 May-3 June, 2017 in Sunny Beach, Bulgaria, edited by K. Georgieva, B. Kirov and D. Danov, ISSN 2367-7570, 66–69.

Miteva, R.; Danov, D.: 2018, Tenth Workshop 'Solar Influences on the Magnetosphere, Ionosphere and Atmosphere', proceedings of the conference held 4-8 June, 2018 in Primorsko, Bulgaria, edited by K. Georgieva, B. Kirov and D. Danov, ISSN 2367-7570, 99–104.

Reames, D. V.: 1999, *Space Science Reviews*, **90 (3/4)**, 413–491

Torsti, J., Valtonen, E., Lumme, M., Peltonen, P., Eronen, T., Louhola, M. et al.: 1995, *Solar Physics*, **162 (1/2)**, 505–531.

Trottet, G., Samwel, S., Klein, K.-L., Dudok de Wit, T., Miteva, R.: 2015, *Solar Physics*, **290 (3),** 819–839

Veronig, A. M., Brown, J. C., Dennis, B. R., Schwartz, R. A.; Sui, L., Tolbert, A. K.: 2005, *The Astrophysical Journal*, **621 (1)**, 482–497

Wall, J. V., Jenkins, C. R.: 2003, *Practical statistics for astronomers*, Cambridge observing handbooks for research astronomers, Vol. 3, Cambridge University Press.